Scanning Electrochemical Microscopy. 31. Application of SECM to the Study of Charge Transfer Processes at the Liquid/Liquid Interface

Chang Wei and Allen J. Bard*

Department of Chemistry and Biochemistry, The University of Texas at Austin, Austin, Texas 78712

Michael V. Mirkin*

Department of Chemistry and Biochemistry, Queens College−CUNY, Flushing, New York 11367

Received: May 8, 1995[⊗]

The kinetics of the electron transfer and ion transfer at the interface between two immiscible electrolyte solutions (ITIES) were probed directly by scanning electrochemical microscopy (SECM). The liquid/liquid (i.e., water/nitrobenzene) interface appeared to be sharp and wave-free on the submicrometer scale. The use of SECM allowed the electron transfer between ferrocene species in nitrobenzene and other redox species in the aqueous phase to be quantitatively separated from the ion transfer processes. The rate constants were extracted from the dependence of the steady-state current at a micrometer-sized tip electrode on the distance between the tip and the phase boundary by comparison to theoretical working curves. In some experiments, the ultramicroelectrode tip penetrating the ITIES trapped a micrometer-thick layer of water inside the nitrobenzene, forming a thin-layer cell.

Introduction

The electrochemistry at the interface between two immiscible electrolyte solutions (ITIES) has been studied extensively during the past two decades.[1] The continuing interest in these systems is due to their relevance to fundamental physicochemical problems (e.g., to homogeneous and heterogeneous electron transfer[2]), electroanalysis,[3] and important technological processes (e.g., solvent extraction in hydrometallurgy[1]). A liquid/liquid interface has been suggested as a simple model for biological and artificial membranes.[4] In electron transfer (ET) theory, the liquid/liquid interface is a very interesting intermediate case linking homogeneous and heterogeneous ET.[1,2] While a few theoretical models of this process have been proposed,[2,5,6] related experimental studies are scarce.[7−9] This is partially due to the difficulty in designing systems that allow clear discrimination between ET and ion transfer (IT) and to the limited potential window for studying ET in the absence of currents controlled by IT. Moreover, the experimental problems typical for conventional measurements of ET at a metal/electrolyte interface are even more severe in the case of ITIES. For instance, it is hard to eliminate the contributions of resistance (the *iR*-drop effect to the measured potential) in highly resistive nonaqueous solvents.

Faradaic and nonfaradaic processes at a metal/liquid interface produce electrical signals that can be directly measured by various electrochemical methods, but analogous processes occurring at the ITIES are less directly accessible by electrochemical measurements.[1] A conventional electrochemical experiment with an ITIES is based on a four-electrode configuration, with reference and auxiliary electrodes positioned in both liquid phases.[10] A four-electrode potentiostat is used to apply a voltage between the reference electrodes and to measure the current flowing between the auxiliary electrodes. The interfacial charge transfer is assumed to be rate limiting, and the whole potential drop is assumed to occur across the interface. However, the ITIES in such an experiment is not microscopically probed directly, and the extraction of mechanistic information from the measured current is not straightforward.

We report here the direct probing of the ITIES by an ultramicroelectrode (UME) used as the tip in the scanning electrochemical microscope (SECM).[11] In the feedback mode of SECM (Figure 1A), a tip UME with a radius a is placed in an aqueous solution containing the reduced form of the redox species, R_1. When the tip is held at a positive potential (with respect to a reference electrode in the aqueous phase), R_1 reacts at the tip surface to produce the oxidized form of the species, O_1. In conventional SECM experiments, when the tip approaches a conductive substrate, the mediator can be regenerated at the substrate and the tip current i_T increases with a decrease in the tip−substrate separation d (positive feedback). At small d the mass transport rate in the gap between the tip and the substrate becomes very high, allowing one to study the kinetics of rapid heterogeneous ET at both tip and substrate electrodes.[11,12] In the experiments described below the water/nitrobenzene interface serves as the equivalent of a conductive substrate, and the regeneration of the mediator occurs via the bimolecular redox reaction between O_1 in the aqueous phase (w) and R_2 in the nitrobenzene (o)

$$O_1(w) + R_2(o) \xrightarrow{k_{12}} R_1(w) + O_2(o) \qquad (1)$$

The kinetics of such a reaction can be evaluated from the tip current. If no regeneration of R_1 occurs, the ITIES blocks mediator diffusion to the tip, so i_T decreases at smaller d; i.e., negative feedback is observed. (Conceptually similar, qualitative SECM studies of electron exchange between a redox couple in solution and another couple confined to a polymer film have been reported.[13]) The collection mode of the SECM (Figure 1B) allows measurement of concentration profiles and monitoring of the diffusion fluxes of electroactive species across the liquid/liquid boundary, as done previously for membranes and various solid targets.[11,14] Another approach to the study of both ET and IT is the SECM thin-layer cell technique,[15] which is based on a formation of a thin (nanometer−micrometer) layer of a liquid inside another liquid phase after the UME tip

[⊗] Abstract published in *Advance ACS Abstracts*, October 1, 1995.

0022-3654/95/2099-16033$09.00/0

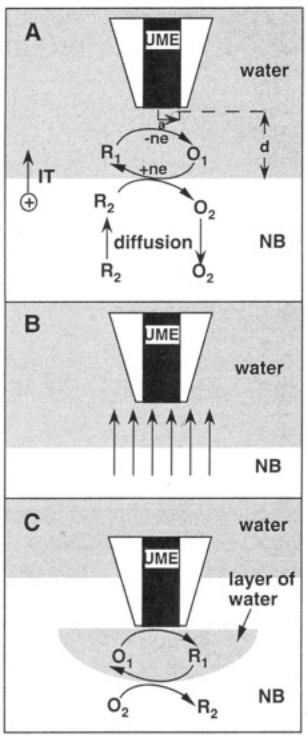

Figure 1. Probing the liquid−liquid interface with the SECM. (A) Measurement of the kinetics of ET between two redox couples confined to different liquid phases with the SECM operating in the conventional feedback mode. Electroneutrality is maintained by IT across the interface. (B) UME tip monitoring ionic fluxes through the interface either potentiometrically or amperometrically. (C) SECM-TLC: a thin-layer cell is formed by trapping a micrometer-thick layer of water between the tip and the NB (the dimensions of the trapped layer are greatly exaggerated in the figure).

penetrates the interface (Figure 1C). The potential advantage of this technique would be the possibility of trapping an extremely thin layer that would allow very fast steady-state measurements. For example, a layer of *o*-dichlorobenzene as thin as 10−20 nm has been trapped inside a Hg pool.[15c]

The use of the SECM eliminates many of the problems that can complicate electrochemical studies of charge transfer processes at the ITIES: (i) The steady-state SECM measurements are essentially free from complications associated with *iR* drop and charging current.[12] (ii) Distinguishing between ET and IT is not a problem because the tip current is clearly due to ET in the feedback mode (Figure 1A) and to IT of tip detectable ions in the collection mode (Figure 1B). (iii) Since the interface does not have to be externally biased, its properties (e.g., thickness) should not change due to the variations in the applied potential, and there are no limitations associated with the polarization window of the ITIES.[1a]

Experimental Section

Chemicals. KCl (J. T. Baker, Phillisburg, NJ), $Ru(bpy)_3Cl_2$ (Strem Chemicals, Newburyport, MA), ferrocene (Fc, Aldrich Chemical Co., Milwaukee, WI), tetraethylammonium perchlorate (TEAP, Sachem, Austin, TX), and nitrobenzene (Mallinckrodt, Paris, KY) were used as received. Sodium ferrocenemonocarboxylate (FcCOONa) was synthesized from ferrocenemonocarboxylic acid (FcCOOH, Strem Chemicals) by reaction with NaOH in methanol and was recrystallized before use. All aqueous solutions were prepared from deionized water (Milli-Q, Millipore Corp.).

Electrodes and Electrochemical Cells. The 10- and 2-μm-diameter Pt wires (Goodfellow, Cambridge, UK) were heat-sealed in glass tubes under vacuum and then beveled to produce SECM tips as described previously.[16] These electrodes were polished with 0.05-μm alumina before each experiment. A three-electrode configuration was employed with a Pt wire (0.5-mm diameter) serving as the counter electrode and 0.5-mm-diameter Ag wire coated with AgCl as the reference electrode. A 5-mL vial mounted on a vibration-isolated horizontal stage was used as the electrochemical cell for SECM measurements. Three milliliters of nitrobenzene (bottom layer) and 1.5 mL of an aqueous solution (top) were poured into the vial to form an ITIES. TEAP was used as the supporting electrolyte for both the organic and aqueous solutions. In some cases, KCl was also used as the supporting electrolyte in the aqueous phase. Both the counter and reference electrodes were in the aqueous phase; however, no appreciable change in SECM response was detected when the counter electrode was immersed in both solutions simultaneously.

SECM Apparatus and Procedure. The basic apparatus used for the SECM experiments has been described previously.[17] Before SECM measurements, the tip electrode was positioned in the aqueous phase and was biased at a potential where the tip process was diffusion-controlled. The approach curves were obtained by moving the tip electrode toward the liquid/liquid interface and recording i_T as a function of d. The data were acquired using software written in-house by D. O. Wipf.

The supporting electrolyte TEAP is soluble in both water and nitrobenzene (NB), and it can partition between the two phases; this could change the concentrations of both TEA^+ and ClO_4^- ions and thus the potential drop across the ITIES.[1] To evaluate the magnitude of this effect, we stirred together equal volumes of water and NB containing equal concentrations of TEAP and left them in a beaker for 24 h. The amount of TEAP found in water and NB after the separation and evaporation of the solvents did not change within experimental error (<5%). Since the aqueous and organic solutions in our experiments were not in contact for more than 1−2 h, TEAP concentration changes due to partitioning were negligible.

Measurement of Formal Potentials. The relative values of the formal potentials of the Fc^+/Fc couple in NB and the $Fc^+COO^-/FcCOO^-$ couple in water were obtained from the cyclic voltammograms at a 5-μm-radius Pt UME vs a Ag/AgCl electrode immersed in the aqueous phase. The cells had the following compositions:

$$\text{Ag/AgCl/H}_2\text{O, 0.1 M TEAP, } 10^{-4}\text{ M KCl, 0.5 mM FcCOO}^-$$

$$\text{Ag/AgCl/H}_2\text{O, 0.1 M TEAP, } 10^{-4}\text{ M KCl//NB, 0.1 M TEAP, 0.5 mM Fc}$$

The 5-μm-radius Pt working and 25-μm-radius counter electrodes were placed in the aqueous phase for $FcCOO^-$ oxidation and in the NB phase for Fc oxidation with the Ag/AgCl reference remaining in the aqueous phase. The measured potential in NB was corrected for the Galvani potential difference ($\Delta_o^w\varphi$) at the liquid junction (//).[1] As discussed below, $\Delta_o^w\varphi$ for 0.1 M TEAP in both phases is −71 mV.

Results and Discussion

Preliminary Characterization of the Interface. The mechanical stability of the liquid/liquid boundary and the accuracy and reproducibility of the data obtained with an ITIES were probed by SECM i_T vs d curves. Previously,[15] a mercury substrate was approached with a micrometer-sized tip in either

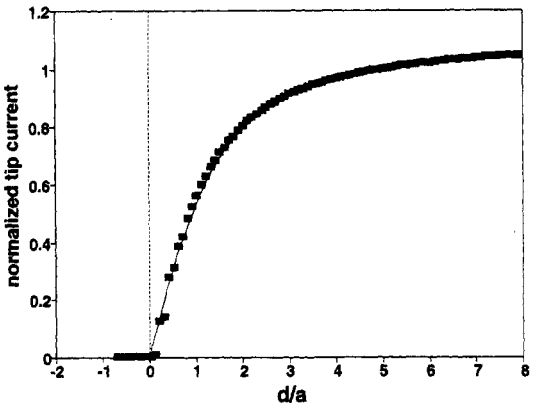

Figure 2. SECM approach curve for a 5-μm-radius Pt tip UME approaching NB from an aqueous solution containing 5 mM FcCOONa and 0.1 M KCl. Positive distances correspond to the tip in water; negative distances correspond to tip penetration into NB. Scan rate was 1 μm/s. The tip potential was held at +400 mV vs Ag/AgCl, sufficiently positive that the oxidation of $FcCOO^-$ was diffusion-controlled. The NB contained no electroactive species, so the interface behaved as an insulator. Solid line represents SECM theory for an insulating substrate.[19]

aqueous or nonaqueous solution, and a considerable level of noise was often observed due to the interfacial vibrations. STM imaging of a Hg surface showed surface waves of ~0.6–0.9 μm in amplitude, in spite of significant efforts to improve stability.[18]

The SECM i_T–d (approach) curve in Figure 2 was obtained with a 5-μm-radius tip immersed in the aqueous solution as it approached the water/NB boundary. The aqueous solution contained 5 mM FcCOONa and 0.1 M KCl, and the NB contained no electroactive species. In this configuration, the NB layer plays the role of an electrical insulator (like glass and Teflon in earlier SECM studies). The tip current decreases with d, because diffusion of the aqueous solution reactant, $FcCOO^-$, to the tip is hindered by the NB layer. Thus, the fit of these experimental i_T–d results to theory and the precision of i_T are an indication of the stability of the interface. The experimental data (squares) represent negative feedback and are in good agreement with the related theory.[19] The tip current is oscillation-free; i.e., any interfacial waves are averaged out or are smaller than ~100 nm in amplitude. The interface is sharp on the submicrometer scale (otherwise, significant deviations from SECM theory would be observed[20]), and the z coordinate corresponding to the zero-distance point can be easily determined. Knowledge of the zero-distance point is essential for quantitative SECM measurements.[11]

When the NB contains a species (Fc) that can react with the tip-generated species ($Ru(bpy)_3^{3+}$), positive feedback occurs as shown in Figure 1A. The positive feedback current in Figure 3 is due to the bimolecular redox reaction

$$Ru(bpy)_3^{3+} + Fc \xrightarrow{k_{12}} Ru(bpy)_3^{2+} + Fc^+ \qquad (2)$$

When the tip penetrates the ITIES ($d = 0$), i_T increases instantaneously and approaches the value expected for a microdisk electrode in a 20 mM Fc in NB solution. The significant difference between the experimental curve (1) and a theoretical curve (2) corresponding to regeneration of the mediator at a diffusion-controlled rate indicates that the process is controlled by interfacial kinetics rather than diffusion.

A complicating factor in this experiment is the possibility of diffusion of Fc and its oxidation product from NB into the aqueous solution and diffusion of the aqueous redox species

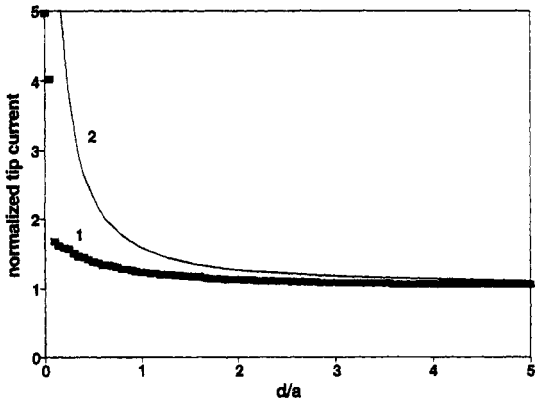

Figure 3. Current–distance curve for a 5-μm-radius Pt tip approaching the water/NB interface (1) and the theory for a diffusion-controlled process (2).[19] Aqueous solution was 5 mM in $Ru(bpy)_3Cl_2$ and 0.1 M in KCl. NB contained 20 mM Fc. The tip current is normalized by $i_{T,\infty} = 4$ nA. The tip potential was +1.1 V vs Ag/AgCl reference.

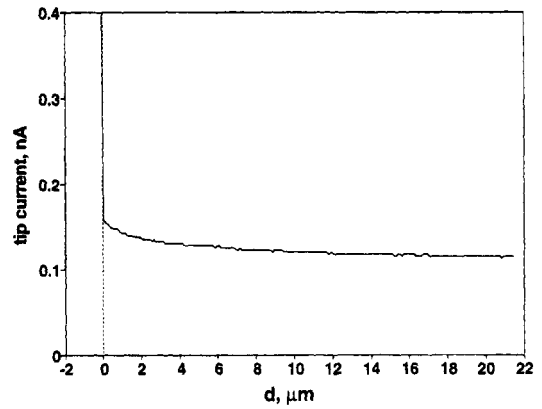

Figure 4. SECM tip approach to the interface between a 0.1 M KCl, 0.1 M TEAP aqueous solution and a 75 mM Fc, 0.1 M TEAP NB solution. Tip current is due to partitioning of Fc from NB into water and the interfacial reaction in eq 3. The tip potential was +1.0 V vs Ag/AgCl reference.

into the NB. Figure 4 contains an i_T–d curve obtained at a 5-μm-radius tip electrode approaching the interface between a 75 mM solution of Fc in NB containing 0.1 M TEAP and an aqueous solution with no redox active species containing 0.1 M KCl and 0.1 M TEAP. As long as the tip is in the aqueous phase, a small steady tip current flows independent of d (i.e., the tip current far from the ITIES, $i_{T,\infty} = 0.117$ nA). This current is caused by the oxidation of a small amount of Fc partitioned into the water from the NB. With a diffusion coefficient of Fc in water of about 1×10^{-5} cm^2/s[21c] and the above value of $i_{T,\infty}$, one can estimate the concentration of Fc in the aqueous solution $c_{Fc,aq}$ to be ~0.06 mM. This corresponds to a distribution coefficient of Fc between NB and water of about 1.2×10^3, somewhat less than 7×10^3,[21b] perhaps because of the presence of electrolyte in our system.

The current in Figure 4 is about 2–10% of a typical i_T measured when a millimolar amount of redox mediator is present in the aqueous phase (e.g., Figure 3). As the tip approaches the interface, within a distance of 3–4 tip radii, i_T increases slightly and a positive feedback current is observed; this is ascribed to the reaction

$$Fc^+(w) + Fc(o) \rightarrow Fc^+(o) + Fc(w) \qquad (3)$$

In the experiment of Figure 3, as long as the concentration of Fc in NB is much higher than that of the redox mediator in water, the main process (i.e., reaction 2) and reaction 3 are completely independent. The contributions of oxidation of the

aqueous mediator ($Ru(bpy)_3^{2+}$) and oxidation of Fc(w) to i_T are thus additive, and the latter can be subtracted from the total measured current as discussed below. When the tip contacts the ITIES, i_T increases instantaneously due to the onset of direct Fc oxidation in NB at the tip.

Measurement of Heterogeneous Kinetics at the ITIES. The measurement of the rate of ET between a component in the aqueous phase and one in the NB is complicated by factors intrinsic to the process itself and those associated with the SECM technique. For example, the driving force for electron transfer includes interfacial potential differences (junction potentials) that are functions of the ionic composition of the phases. In the SECM measurements shown schematically in Figure 1A, four stages of the overall process can affect the tip current: mediator diffusion between the tip and the ITIES, the interfacial reaction (eq 1), diffusion of Fc in NB, and charge compensation by IT. The electrical current across the ITIES (i_S) caused by this multistage serial process can be expressed as[22]

$$1/i_S = 1/i_T^c + 1/i_{ET} + 1/i_d + 1/i_{IT} \quad (4)$$

where i_T^c, i_{ET}, and i_{IT} are the characteristic limiting currents for the above four stages. Any of these stages can be rate limiting, but in our experiments the concentration of Fc was always sufficiently high to exclude the possibility of diffusion limitations in the NB. The portion of the substrate surface (i.e., the portion of the ITIES area) participating in the SECM feedback loop is a disk with a radius somewhat larger than the tip radius.[23] Thus, the lower limit for i_d can be obtained as follows:[24]

$$i_d \geq 4nFaD_{Fc}c_{Fc} \quad (5)$$

where D_{Fc} and c_{Fc} are the diffusion coefficient and the concentration of Fc in NB, respectively. c_{Fc} was ≥ 25 times the concentration of the redox mediator in the aqueous solution, so $i_d \gg i_T^c$ and diffusion in NB could not be the rate-limiting stage.

When the ion transfer is fast, previously developed SECM theory for a process governed by finite irreversible substrate kinetics[11b,20,23] should be applicable to an analysis of the i_T-d curves. Since fitting experimental results to numerical theoretical working curves[23] is time-consuming and sometimes not very accurate, two analytical approximations have been derived;[11b,20] one is suitable for relatively fast kinetics ($I_{T,0} \gtrsim 2$, where $I_{T,0}$ is the normalized tip current, $i_T/i_{T,\infty}$, at $d \rightarrow 0$) and the other for slow kinetics ($I_{T,0} \lesssim 0.5$). However, neither of these can be used to treat the intermediate kinetic region which is important for this study. We have found that the whole family of SECM working curves[23] calculated for $0.1 \leq L \leq 1$ and $-2 \leq \log \kappa \leq 3$ can be accurately described by the equations

$$I_S^k = 0.78377/L(1 + 1/\Lambda) + [0.68 + 0.3315 \exp(-1.0672/L)]/[1 + F(L,\Lambda)] \quad (6a)$$

$$I_T^k = I_S^k(1 - I_T^{ins}/I_T^c) + I_T^{ins} \quad (6b)$$

where I_T^c, I_T^k, and I_T^{ins} represent the normalized tip currents for diffusion-controlled regeneration of a redox mediator, finite substrate kinetics, and insulating substrate (i.e., no mediator regeneration), respectively, at a normalized tip–substrate separation, $L = d/a$. I_S^k is the kinetically controlled substrate current; $\Lambda = k_f d/D_R$, k_f is the apparent heterogeneous rate constant (cm/s), $\kappa = k_f a/D$, D_R is the diffusion coefficient of the reduced mediator in water, and $F(L,\Lambda) = (11 + 7.3\Lambda)/\Lambda/(110 - 40L)$. I_T^c, I_T^k, and I_T^{ins} are normalized by the tip current at an infinite tip–substrate separation, $i_{T,\infty} = 4nFaD_Rc_R$. The analytical approximations for I_T^c and I_T^{ins}

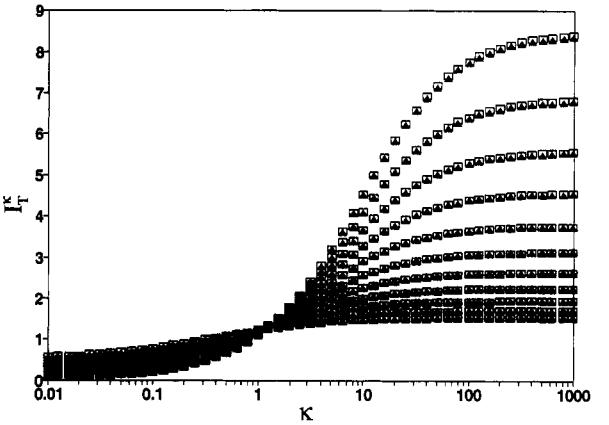

Figure 5. Working curves of I_T^k vs κ for different values of d/a: open squares, eq 6; filled triangles, simulation in ref 23. From top to bottom, $\log(d/a) = -1.0, -0.9, -0.8, -0.7, -0.6, -0.5, -0.4, -0.3, -0.2, -0.1$, and 0.0. $\kappa = k_f a/D$.

$$I_T^c = 0.78377/L + 0.3315 \exp(-1.0672/L) + 0.68 \quad (7)$$

$$I_T^{ins} = 1/(0.15 + 1.5358/L + 0.58 \exp(-1.14/L) + 0.0908 \exp[(L - 6.3)/(1.017L)]) \quad (8)$$

have been derived previously.[25] Figure 5 gives the family of working curves I_T^k vs κ for different values of L along with the simulated data from ref 23. The numerical results (triangles) fit eq 6 (squares) within ~1–2%, which is smaller than the experimental uncertainty. Since I_S^k represents a combination of diffusion in the aqueous phase and finite kinetics of ET

$$1/I_S^k = 1/I_T^c + 1/I_{ET} \quad (9)$$

where

$$i_{ET} = nFAk_f c_R \quad (10)$$

and $I_{ET} = i_{ET}/i_{T,\infty}$. Equation 4 may be simplified, and the tip current vs distance curves can be obtained using eqs 11 and 12

$$1/I_S = 1/I_S^k + 1/I_d + 1/I_{IT} \quad (11)$$

$$I_T = I_S(1 - I_T^{ins}/I_T^c) + I_T^{ins} \quad (12)$$

Separation of ET from IT. In most previous studies of liquid/liquid interfaces carried out at either macro- or micro-ITIES, the same interface area was available for both ET and IT processes. In contrast, the ET process in SECM experiments occurs at a micrometer-size area of the ITIES confronting the tip, while IT can occur at any point on the large (on the order of cm^2) phase boundary. While this observation might suggest that IT limitations may be unimportant under suitable experimental conditions, a careful kinetic analysis is always necessary to identify the rate-limiting stage. For example, the differences between curves 1 and 2 in Figure 3 could be attributed to finite ET kinetics, and using the above theory, one could calculate k_f from curve 1. However, this result would not be reliable. The ET in reaction 2 should be quite fast because of the large driving force (the standard potentials of the two redox couples differ by almost 1 V) and the large self-exchange rate constants. In contrast, IT may be quiet slow, since the NB contained no supporting electrolyte, and thus IT is likely to be the rate-limiting stage.

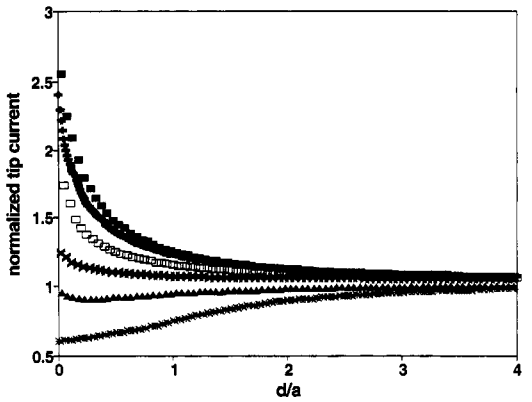

Figure 6. Effect of the concentration of FcCOONa in the aqueous phase on the shape of current–distance curves. $c_{FcCOONa}$ was, from top to bottom, 0.25, 0.5, 0.8, 1.0, 2.0, and 5.0 mM. Aqueous solution also contained 0.1 M KCl; NB contained 75 mM Fc.

We investigated the possibility of separating the ET and IT processes using the slower reaction between Fc in NB and FcCOONa in water

$$FcCOO^-(w) - 1e^- \rightarrow FcCOO(w) \quad \text{(tip)} \quad \text{(13a)}$$

$$Fc(o) + FcCOO(w) \rightarrow Fc^+(o) + FcCOO^-(w) \quad \text{(ITIES)} \quad \text{(13b)}$$

From Figure 6 one can see that in the absence of supporting electrolyte in NB the normalized tip current decreases markedly with an increase in the concentration of FcCOONa in water ($c_{FcCOONa}$). This cannot be attributed to ET limitations, because the rate of the ET is proportional to $c_{FcCOONa}$ according to eq 10 (where R = $FcCOO^-$). The shapes of the approach curves in Figure 6 also differ from those typical for finite ET kinetics. For example, in the second and the third curves from the bottom, one can detect a shallow minimum that is inconsistent with slow ET.[20,23] According eq 6, a decrease in k_f causes the appearance of a maximum in all current–distance curves with $0.5 < I_{T,0} < 1.5$. That is, finite ET kinetics at the interface first causes an increase in tip current because of positive feedback before a decrease caused by blocking effects as the tip approaches the interface.[17,23] Since no such maximum was observed in our experiments, the shape of the current–distance curves in Figure 6 cannot be explained by a change in k_f. Further evidence of IT limitations comes from the pronounced dependence of the shape of the i_T–d curves upon the concentration of TEAP c_{TEAP} (equal in both phases, Figure 7). The normalized feedback current increases markedly with an increase in c_{TEAP} up to ~10 mM. At higher values, the shape of the current–distance curves becomes independent of c_{TEAP}, so that the two upper curves in Figure 7 (shown by pluses and squares) obtained with 10 and 75 mM TEAP, respectively, are practically indistinguishable. Importantly, at this concentration of supporting electrolyte, the normalized tip current also became independent of $c_{FcCOONa}$. Thus, at $c_{TEAP} > 10$ mM and $c_{FcCOONa} \leq 1$ mM the overall process is limited by slow ET, and the related rate constant can be extracted from experimental i_T–d curves fit to eq 6b. Such curves obtained at different concentrations of Fc in NB with $c_{TEAP} = 0.1$ M and $c_{FcCOONa} = 0.5$ mM are shown in Figure 8. The solid lines in Figure 8 represent theoretical curves calculated with different k_f values (0.02–0.06 cm/s) corresponding to different concentrations of Fc in NB (Figure 9). The k_f values were computed from the related values of κ with the diffusion coefficient of $FcCOO^-$ in water of 5.8×10^{-6} cm^2/s found from steady-state voltammetry. The reaction between Fc and FcCOO was treated as an irreversible process in spite of the very small

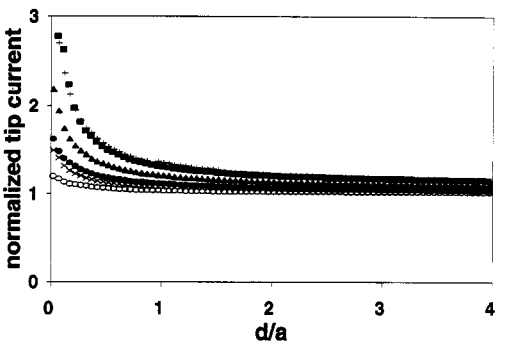

Figure 7. Effect of the concentration of TEAP on the shape of current–distance curves. The concentration of TEAP in both NB and water was (○) 0, (×) 0.01, (●) 0.1, (▲) 1, (■) 10, and (+) 75 mM. Aqueous solution also contained 1 mM FcCOONa and 0.1 M KCl; NB contained 75 mM Fc.

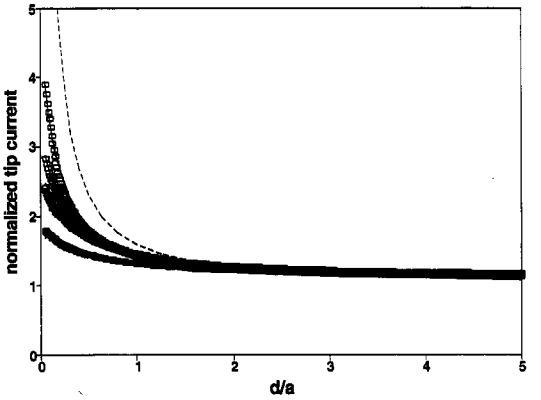

Figure 8. Approach curves obtained at different concentrations of Fc in NB and with a large excess of supporting electrolyte. From bottom to top c_{Fc} was 20, 50, 75, and 100 mM; $c_{FcCOO^-} = 0.5$ mM; $c_{TEAP} = 0.1$ M. $I_{T,\infty}$ for all curves was about 1 nA. Solid lines calculated from eq 6. See Figure 9 for rate constant values. Dashed line represents the theory for a diffusion-controlled process.[19]

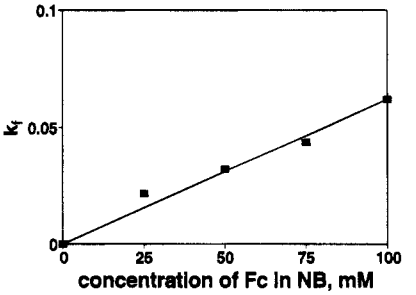

Figure 9. Apparent heterogeneous rate constant as a function of concentration of Fc in NB. The k_f values were calculated from the approach curves in Figure 8 with $a = 5$ μm and $D_{FcCOO^-} = 5.8 \times 10^{-6}$ cm^2/s.

difference in standard potentials of the two redox couples. (The $E°$ of Fc^+/Fc in NB is about 50 mV more positive than that of $FcCOO/FcCOO^-$ in water when measured against the same reference electrode immersed in the aqueous phase, with correction for the $\Delta_o^w\varphi$,[26] as discussed in the Experimental Section.) This was possible because of a large and essentially constant value of c_{Fc} in NB leading to $c_{Fc,NB}c_{FcCOO,aq} \gg c_{Fc^+,NB}c_{FcCOO^-,aq}$ in the interfacial region.

As stated above, the oxidation of any Fc partitioned from NB into water (Figure 4) could contribute up to 10% to the tip current. This current could be subtracted point by point from the corresponding approach curve; for example, the i_T–d curve presented in Figure 4 could be subtracted from the second from the top curve in Figure 8 obtained with the same concentration

of Fc in NB (75 mM). Our calculations showed that such a subtraction would cause the k_f values to be about 10% higher than those in Figure 9. Since this is not much larger than our experimental error, the original experimental data without subtraction of the Fc background are shown.

Since the NB and water contained only the reduced forms of Fc and $FcCOO^-$, respectively, the ITIES was not poised by a redox equilibrium. Thus, the $\Delta_o^w\varphi$ was governed by concentrations of potential-determining ions (TEA^+ and ClO_4^-) in both phases.[1] The concentration of both ions was 0.1 M for all approach curves in Figure 8 and was more than 100 times higher than the concentrations of any other charge species, excluding nonpartitioning K^+ and Cl^-. Therefore, the potential drop across the ITIES did not change significantly from one curve to another, and k_f was not affected by a change in the driving force. One needs to know $\Delta_o^w\varphi$ to compare these results to previously reported data and theory. This can be evaluated as[27]

$$\Delta_o^w\varphi = 0.5(\Delta_o^w\varphi^\circ_{TEA^+} + \Delta_o^w\varphi^\circ_{ClO_4^-}) \quad (14)$$

where $\Delta_o^w\varphi^\circ_{TEA^+}$ and $\Delta_o^w\varphi^\circ_{ClO_4^-}$ are the standard Galvani potential differences for the TEA^+ and ClO_4^- ions, respectively. Using the ΔG_p values tabulated for these ions in ref 1a (we have used the standard energy of partition, ΔG_p, rather than the standard energy of transfer, ΔG_t, assuming that both water and NB were saturated with the other solvent), one can obtain from eq 14 $\Delta_o^w\varphi = -71$ mV. Since the difference between the standard potentials of $Fc^{+/0}$ and $FcCOO^{0/-}$ is small (the first redox couple is about 50 mV more positive), the $\Delta_o^w\varphi$ corresponding to a zero driving force for this reaction should be very close to 0 V, and the standard rate constant k° in 100 mM of Fc is perhaps somewhat more than 0.1 cm/s. This can be compared to the previously reported value of $k^\circ = 9 \times 10^{-4}$ cm/s for the lutetium biphthalocyanine $[Lu(PC)_2]$ and $Fe(CN)_3^-$ couple.[9a] The latter value was extracted from cyclic voltammograms using the Nicholson method.[28] Aside from the possible influence of charging current and resistive potential drop (suggested by the shape of cyclic voltammograms in Figure 3 of ref 9a), this difference may be attributed to the (i) slower kinetics of the $Fe(CN)_6^{3-/4-}$ couple, (ii) relatively high solubility of Fc in water, (iii) double-layer effects, and (iv) possible inapplicability of the Nicholson method, and even the Butler–Volmer formalism in general, to ET at the ITIES. The slow heterogeneous kinetics of $Fe(CN)_6^{3-/4-}$ may also arise from surface effects rather than the intrinsic sluggishness of ET,[29] and very little is known about the dependence of k_f at the ITIES on either interface structure or potential.

The above rate constant could be compared more easily to that obtained for the self-exchange reaction (eq 3), since both processes were studied under nearly the same conditions (i.e., solvents, electrolytes, concentrations, interfacial potential drop) and by the same technique. Since the driving forces and self-exchange constants for these two reactions were very similar, one could expect to see similar rate constants as well. Although we did not carry out a detailed kinetic analysis of the Fc/Fc^+ reaction, from the shape of the approach curves one can see that the rates of ET are of the same order of magnitude. The ET between Fc and $Ru(bpy)_3^{3+}$ is significantly faster due to the large difference in the driving force (i.e., standard potentials of the half-reactions). Quantitative comparison was difficult because the latter reaction could not be studied with TEAP as the supporting electrolyte, since ClO_4^- forms an insoluble product with the ruthenium species.

Bimolecular Rate Constant of the ET. A bimolecular rate constant, k_{12}, of 0.6 M^{-1} cm s^{-1} can be obtained from the linear dependence of k_f vs c_{Fc} (Figure 9) and can be used to quantitatively express the rate of the interfacial ET in a form that can be compared to theoretical models.[2] The computed value of k_{12} depends on the physical model adopted. There is no consensus in the literature about the most appropriate model because of lack of information about the structure and thickness of the liquid/liquid interface and potential profiles in the ITIES.[30-32] Thus, one can calculate k_{12} either by assuming a sharp, planar boundary between the two solvents[2b] or by adopting a reaction-layer-type formalism.[2d] The former approach leads to the following equation[2b-d] for an ET reaction between reactant 1 in solvent 1 and reactant 2 in solvent 2.

$$k_{12} = [2\pi(a_1 + a_2)\Delta R/\kappa\nu]k_1^{el}k_2^{el}\exp[-(\Delta G^\circ/2k_BT) - (\Delta G^{\circ 2}/4\lambda k_BT)] \quad (15)$$

where k_{12} is the interfacial ET rate constant under the conditions that the driving force is the difference in free energy between redox couples 1 and 2 and any additional applied potential across the interface (ΔG°), a_1 and a_2 are the radii of the two reactants, ΔR is the ET parameter ~1 Å, k_1^{el} and k_2^{el} are the standard heterogeneous outer-sphere ET rate constants for the two redox couples at a metal electrode (cm/s) in solvents 1 and 2, $\kappa\nu$ is the product of the adiabaticity factor and the nuclear motion frequency, and λ is the reorganization energy. The special case considered in previous theoretical treatments[2] pertained to the exchange current rate constant, k_{12}, at zero driving force (equivalent to eq 15 with $\Delta G^\circ = 0$). To express k_{12} in units of M^{-1} cm s^{-1} (used in ref 2), the right-hand side of eq 15 must be multiplied by 6.02×10^{20}.[2e] Multiplication of the right-hand side of eq 15 by the constant factor $0.5\ (a_1 + a_2)^2/(\Delta R)^2$ [2a] leads to the applicable equation when reactants partially penetrate the phase boundary to the extent that their centers can reach the interfacial plane. Multiplication by another factor of 2 $(a_1 + a_2)L/(\Delta R)^2$ yields the applicable equation for a fairly thick interface (e.g., a thickness of the boundary layer $L \approx a_1 + a_2 \approx 1$ nm).[2b,d] When the driving force is not very large (e.g., $|\Delta G^\circ| < 0.15$ eV), all of these cases can be represented as

$$k_{12} = [4\pi(a_1 + a_2)^2L/\Delta R\kappa\nu]k_1^{el}k_2^{el}\exp[-(\Delta G^\circ/2k_BT)] \quad (16)$$

where the effective thickness of the reaction layer L is equal to $0.5\ (\Delta R)^2/(a_1 + a_2)$ for an infinitely thin boundary and $(a_1 + a_2)/4$ for half-penetration, and it represents the actual thickness of the layer when it is a few solvent molecules thick.

In refs 2b and 2d the theory developed was compared to the experimental rate constant from ref 9a. The k_{12} was calculated for a special value of the potential drop across the ITIES corresponding to a zero driving force ($\Delta G^\circ = 0$). A Butler–Volmer-type dependence of the ET rate constant upon the applied potential was assumed, although such a dependence has not been demonstrated for ET at the ITIES. Since the interface thickness and phsyical localization of the ET reaction are unknown, one cannot evaluate the local potential for either of the reactants. Moreover, if the ET occurs in a finite reaction layer which does not coincide with the mixed solvent layer, there may be essentially no potential drop in a reaction layer, and so the k_{12} may be potential independent (as suggested for the IT rate constant[33]). The apparent potential dependence of the process rate in this case could arise from a change in the surface concentrations of the reactants. (The potential dependence of k_{12} can be studied by changing the ratio of concentrations of the potential-determining ions or by applying an external potential across the interface to produce a potential drop $\Delta_o^w\varphi$. Such experiments are underway in our laboratories.) A

more precise value of k_{12} can probably be obtained without application of an external bias to the ITIES. If the concentrations of the potential-determining ions in both solvents are chosen such that $\Delta_o^w\varphi$ is about zero, the driving force in eq 16 represents the difference between the standard potentials of the two couples, $\Delta G^\circ = -nF\Delta E^\circ$. Alternatively, at zero $\Delta_o^w\varphi$, k_{12} can be calculated from eq 17 which follows from eq 13 in ref 2d and eqs 96 and 97 in ref 34.

$$k_{12} = L\sqrt{k_{11}k_{22}K_{12}f} \tag{17}$$

where $K_{12} = \exp(-nF\Delta E^\circ/RT)$ is the equilibrium constant for reaction 1, ΔE° is the difference between the two standard potentials, k_{11} and k_{22} are the self-exchange rate constants for the two redox couples in solvents 1 and 2, respectively, and $\log f = (\log K_{12})^2/(4\log(k_{11}k_{22}/Z_{soln}^2)$; Z_{soln} is the collision frequency. The dependence of the ET rate on ΔE° is not apparent from the voltammetric results in ref 9a, since one phase in that study contained concentrated redox species and showed a metal-like behavior.

Two theoretical values of k_{12} were computed in ref 2d; one assumed an infinitely thin interface (eq 15 with $\Delta G^\circ = 0$), and the other assumed a reaction layer thickness of 10 Å. After multiplication by a factor of 10^{-3},[2e] the first value appears to be more than 3 orders of magnitude lower than the experimental value.[9a] The second value is about 25 times lower; i.e., the agreement with the experimental value could be achieved assuming $L = 25$ nm. Note, however, that both theoretical values were obtained by assuming a value for the standard electrochemical rate constant for $Lu(PC)_2$ of 200 cm/s. Such a high value was never obtained experimentally and was based on rate constants of the same order of magnitude reported for several other outer-sphere ET reactions.[35] The validity of those results, however, has been questioned.[36] If a more conventional value of k^{el} for $Lu(PC)_2$, i.e., about 1 cm/s is assumed, one would need an $L = 5$ μm.

From the slope of the straight line in Figure 9 one can find $k_{12} = 0.6$ M^{-1} cm s^{-1}. For our conditions, $\Delta E^\circ = 50$ mV and $\Delta_o^w\varphi = -71$ mV, so the total driving force for a is 0.12 eV and the exponential term in eq 16 is of the order of 0.1. We evaluated k_1^{el} and k_2^{el} for the oxidation of Fc in NB and $FcCOO^-$ in water from steady-state voltammetry at 1-μm- and ~30-nm-radius Pt microelectrodes.[37] Both rate constants were of the order of 1 cm/s. With these values and $a_1 = a_2 = 3.8$ Å for Fc,[38] and with $FcCOO^-$ and other parameters from refs 2b and 2d, from eq 16 we obtain k_{12} (M^{-1} cm s^{-1}) = $440L$. Thus, an agreement with the experimental results would require L to be somewhat larger than 10 μm. A completely different result can be obtained from eq 17. Taking $k_{11} = 3.0 \times 10^7$ M^{-1} s^{-1} for Fc in NB[38] and assuming the same value for k_{22} (which seems to be reasonable because of the similarity of electrochemical rate constants), one can obtain k_{12} (M^{-1} cm s^{-1}) ≅ $3 \times 10^{+6}L$. Comparison with the above experimental value leads to $L = 2$ nm.

Since the Fc species can penetrate the interface and its distribution coefficient between water and NB is not negligible, the assumption of the ET occurring at an infinitely thin phase boundary is implausible. Thus, one should account for two reaction layers formed on both sides of the interface. For simplicity, let us consider only one reaction layer of Fc in water. The upper limit for the thickness of the reaction–diffusion layer, μ, can be evaluated from the value of k_f[39]

$$\mu = KD_{Fc,aq}/k_f \tag{18}$$

where K is the ratio of the concentration of Fc in water and in NB, i.e., about 8×10^{-4} (see above), and the diffusion coefficient of Fc in water, $D_{Fc,aq} \cong 10^{-5}$ cm^2/s.[21] For k_f in the range 0.02–0.05 cm/s (Figure 9), one obtains a μ of 2–4 nm. The L value found from eq 17 fits into this range. The apparent difference between this result and the L value obtained from eq 16 is probably of the same nature as the differences between theoretically predicted and experimentally measured electrochemical rate constants for outer-sphere ET. SECM experiments are currently under way to determine the interface thickness. However, preliminary results suggest that this is of the order of a few nanometers. Figure 10 shows the approach curve of a 25-nm Pt tip moved through the interface from an aqueous solution into a 10 mM Fc, NB solution. The tip current shows that a transition from the near-zero level in the aqueous phase to the level in NB occurred over a distance of ≤4 nm. Note that under the conditions of this experiment essentially no current attributable to Fc oxidation in the aqueous phase was observed.

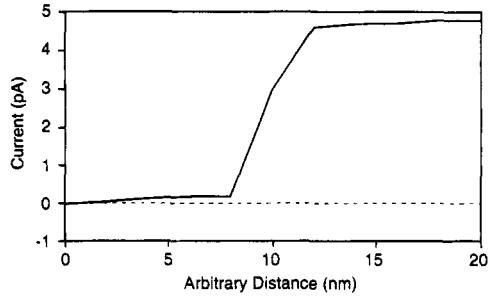

Figure 10. Current–distance curve for 25-nm-radius Pt tip moved perpendicular to and through the interface: H_2O, 0.1 M TEAP//NB, 0.1 M TEAP, 10 mM Fc. The tip potential was held at 0.5 V vs Ag quasi-reference electrode, and the tip was scanned at 20 nm/s.

Ion Transfer. Since the redox process in NB is oxidation, the injected positive charges must be compensated by either cation expulsion from or anion injection into the NB. With no excess of supporting electrolyte in NB, the overall process should be under mixed ET and IT kinetic control. This situation is somewhat different from those discussed in the literature[1] where the IT process was driven by potential drop across the ITIES. To our knowledge, no theoretical treatment has been proposed for IT at the ITIES induced by ET. The exact formulation of this problem is difficult and beyond the scope of this paper. We thus try to investigate the IT limitations by deriving an empirical approximation for the I_{IT} term in eq 11.

In the absence of TEAP, the charge compensation by anion movement should not be significant, because aqueous Cl^- does not transfer readily into NB ($\Delta G_p = 43$ kJ/mol),[40] and charge compensation would mainly occur by transfer of Fc^+ from NB into water.[21] Note, however, that the total number of Fc^+ ions produced by ET at the interface is just sufficient to compensate for the positive charge injection into the NB. Since there is a finite probability that the newly formed Fc^+ diffuses into the bulk NB instead of crossing the ITIES, another IT process should occur to maintain electroneutrality. Of the two anions present in water, Cl^- and $FcCOO^-$, Cl^- IT is probably favored, because its concentration is about 100 times that of $FcCOO^-$, and we were unable to detect any amount of $FcCOO^-$ in the NB (see Figure 2). Thus, we represent the limiting IT current as a sum of two terms: one for the transfer of Fc^+, taken to be proportional to the concentration of Fc^+ at the interface, and the second for the transfer of Cl^- or $FcCOO^-$ from water to NB (as well as the transport of charged impurities) as independent of c_{Fc^+}.

$$i_{IT} = ac_{Fc^+} + b \tag{19}$$

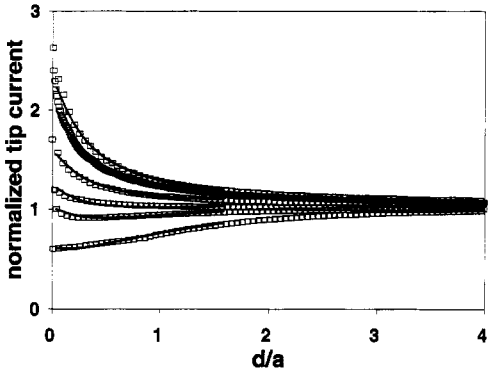

Figure 11. Current−distance curves obtained with different concentrations of FcCOONa and no supporting electrolyte in NB fit to theory (eqs 11, 12, and 20) with the adjustable parameters A and B. The theoretical curves were calculated for normalized distances up to $d/a = 1.6$ because of the limitations of the approximation (eq 6). $A = 0.28$. See Figure 6 for experimental parameters and Figure 12 for B values.

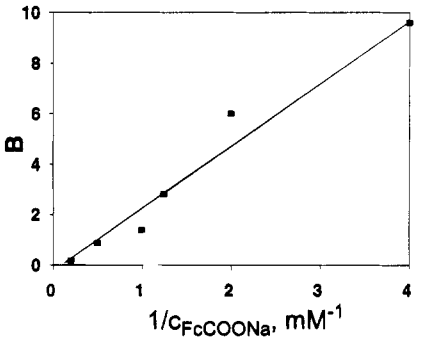

Figure 12. Dependence of the parameter B from eq 20 vs $1/c_{FcCOONa}$. Points represent the B values used to fit the experimental current−distance curves in Figure 11.

where a and b are empirical constants. Since the SECM feedback current, I_S in eq 11, is proportional to c_{Fc^+} at the interface, one can rewrite eq 19 for the normalized current I_{IT}

$$I_{IT} = A/(1/I_S^{\,k} + 1/I_d) + B \qquad (20)$$

where A and B are dimensionless empirical parameters. A should be independent of aqueous mediator concentration, and B is expected to be inversely proportional to $c_{FcCOONa}$. We found it possible to fit all of the approach curves in Figure 11 using eqs 11, 12, and 20 with a fixed value of A and with B increasing monotonically with a decrease in $c_{FcCOONa}$. This is not trivial because the curvature of the lower curves is significantly different from that of the usual SECM approach curves. The dependence of B vs $1/c_{FcCOONa}$ obtained (Figure 12) is essentially linear, and the correlation is quite good for such a simple model.

To fit the approach curves obtained with different concentrations of TEAP in both solvents, the expression for I_{IT} should also account for the contribution of TEAP to the IT. Since the concentrations of TEA^+ and ClO_4^- were the same in both phases, a single term proportional to c_{TEAP} must be added to eq 20

$$I_{IT} = A'/(1/I_S^{\,k} + 1/I_d) + B' + Gc_{TEAP} \qquad (21)$$

where G is another adjustable parameter. From Figure 7 one can see that the addition of even a small amount of TEAP to both solvents (e.g., $c_{TEAP} = 0.01$ mM in Figure 7, 100 times lower than $c_{FcCOONa}$) produces a considerable increase in the tip current. Above this level, the feedback current increased only marginally upon the increase of TEAP by the factor of 10

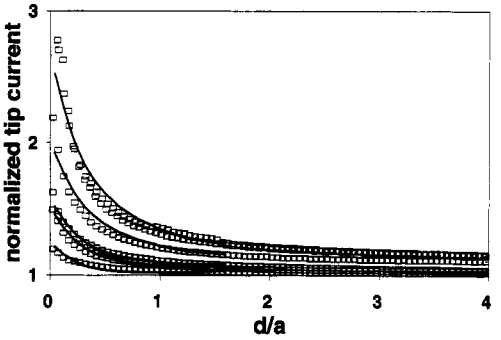

Figure 13. Current−distance curves obtained with different concentrations of TEAP in NB and water. Theoretical curves (solid) were obtained using eqs 11, 12, and 21 with the values of A', B', and G given in the text. See Figure 7 for experimental parameters.

(0.1 mM), but additions of TEAP to 1 and 10 mM again resulted in significant increases in I_{IT} (and thus in I_T). These findings suggest that the initial increase in I_{IT} was most likely caused not by a direct contribution of the added TEAP to IT ($c_{TEAP} = 0.01$ mM was probably too small for that), but rather by a change in the potential drop across the ITIES. Such a change apparently increased the values of A and B, which are proportional to the potential-dependent IT rate constants. Subsequent changes in c_{TEAP} should not have significantly affected $\Delta_o^w\varphi$, because the ratio $c_{TEAP,aq}/c_{TEAP,NB}$ remained constant. The whole family of approach curves in Figure 11 was fit using $A = 0.28$ and $B = 1.39$ for the lower curve (these values were obtained from the fit in Figure 11 for $c_{FcCOONa} = 1$ mM and no TEAP in either solvent) and the somewhat higher values of $A' = 0.54$ and $B' = 1.5$ for all of the other curves obtained with different concentrations of TEAP and $G = 3500$. Combining eq 21 with eqs 11 and 12, one can fit all of the approach curves and predict the saturation effect observed at $c_{TEAP} > 0.01$ M (Figure 13). Although this simple formalism was surprisingly successful in a quantitative description of the IT process, additional efforts are needed to develop an exact model and to extract the IT rate constant from the SECM data. This kind of ET/IT coupling should be equally important for heterogeneous processes at the polymer film/solution interface. In hydrophilic polymers, a change in the interfacial potential drop is one factor causing a breaking-in or first-cycle effect,[41] while in hydrophobic polymers IT should always affect the electrochemical measurements. The ITIES is more convenient for studying such complex processes compared to polymer films, because the interfacial composition and structure (e.g., interface area) should be better defined.

Thin-Layer Cell Formation. An i_T-d curve that differed markedly from those previously shown was found in a few experiments (Figure 14). Although at longer distances i_T grew exponentially with a decrease in d, in accord with known SECM theory,[11] at $d \cong 0$, where the tip should penetrate the water/NB interface, there was a point of inflection after which the tip current leveled off. In this regime, the measured i_T always remained much lower than it would have been with the tip immersed directly in NB (i.e., $i_d = 80$ nA), showing that direct contact between the tip and organic solvent had not occurred. Similar types of i_T-d curves were obtained previously in SECM experiments with a mercury pool substrate[15] and were explained by the trapping of a thin (nanometer−micrometer) layer of electrolyte inside the Hg pool after the tip pushed into the Hg surface. Analogously, in Figure 14 the UME tip at the ITIES traps a micrometer-thick layer of water inside the NB (Figure 1C). This tip/water/nitrobenzene configuration behaves like a twin-electrode thin-layer cell (TLC) whose thickness (~1.3 μm) can be evaluated from i_T. Electrochemical measurements inside such a TLC, e.g., steady-state voltammetry, can yield kinetic

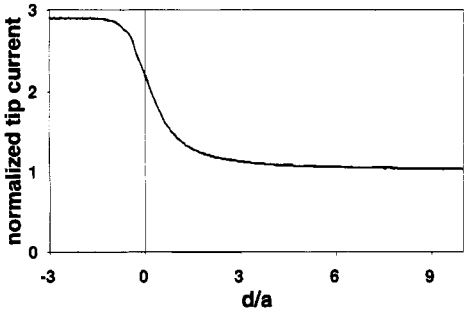

Figure 14. Current−distance curve for a 5-μm-radius Pt tip approaching the water/NB interface. The solutions contained 0.5 mM FcCOONa, 0.1 M TEAP (water) and 80 mM Fc, 0.1 M TEAP (NB). Positive distances correspond to the tip approaching the phase boundary; negative distances correspond to thin-layer formation in NB.

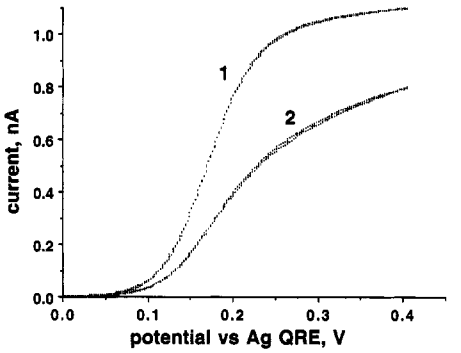

Figure 15. Steady-state voltammograms of oxidation of Fc in NB at a 1-μm-radius Pt tip electrode (1) immersed directly into NB and (2) preimmersed in an aqueous solution. v = 5 mV/s. NB contained 5 mM Fc and 0.1 M TEAP. Potential was measured vs Ag quasi-reference electrode.

and thermodynamic parameters for the related redox reaction.[15] Further studies of the trapping mechanism are needed to identify conditions influencing thin-layer formation and to find those that will decrease the thickness of the trapped layer to the more useful nanometer range. This phenomenon might also be explored as a very simple method of electrode modification with a thin liquid layer, for example, to prevent electrode fouling when carrying out voltammetric analysis in biological media.

Nakatani et al.[21] recently reported somewhat similar electrochemical measurements in a laser-trapped droplet of oil in water. Such drops were brought into contact with a 10-μm-wide gold microband electrode. The oxidation of Fc inside a drop of NB at a Au electrode appeared to be irreversible with a standard rate constant $k^{el} \leq 10^{-3}$ cm/s and a transfer coefficient α = 0.1 as extracted from cyclic voltammograms.[21b] The authors explained this apparent irreversibility by passivation of the electrode surface by a water layer adsorbed before the oil droplet was placed onto the Au band surface. Figure 15 contains two voltammograms of Fc in NB; curve 1 was obtained at a 1-μm-radius Pt disk electrode immersed directly into NB, and curve 2 was obtained with the same electrode preimmersed in an aqueous solution. Curve 2 indeed shows a slower rate of Fc oxidation (although the rate constant seems to be higher than the values suggested in ref 21b); however, an even more prominent effect is the decrease in the plateau current. This cannot be explained by passivation, i.e., adsorption of a monolayer of water, but rather suggests trapping of a thin layer of water between Pt and NB. A concentration of Fc in such a layer of ~50−100 μM is sufficiently high to sustain the measured current (nanoampere range) if its thickness is of the order of 10−50 nm. Analogously, when the SECM tip penetrates NB without any indication of thin-layer trapping, it does not necessarily mean that the tip surface is completely free of water, because such a layer may be too thin to influence the shape of the approach curve.

Conclusions

We have described the SECM-based procedure for investigation of charge transfer processes occurring at the ITIES, i.e., ET via a bimolecular reaction between redox species confined to different solvents and the IT process maintaining electroneutrality. The interface between water and NB was found to be mechanically stable and sharp on a submicrometer scale. The UME tip probed the interface directly, allowing effective separation of ET from IT. Kinetic limitations associated with slow IT can be quantitatively described by an approximate linear model. The effective heterogeneous rate constant for ET between Fc and FcCOONa at a constant Galvani potential difference ($\Delta_o^w\varphi$ = −71 mV) was directly proportional to the concentration of Fc in NB. The corresponding bimolecular rate constant was about 0.6 M^{-1} cm s^{-1}. The agreement between this value and the theoretical value obtained using the Marcus formula, eq 17, can be achieved by assuming an interface thickness of 2 nm.

While conventional studies of the ITIES have been carried out at externally biased polarizable ITIES, in SECM measurements a nonpolarizable ITIES is poised by the concentrations of the potential-determining ions providing a constant driving force for the ET and IT processes. The driving force can be changed by varying the $\Delta_o^w\varphi$, and the potential dependence of the ET rate constant can be studied. It should be possible to carry out such measurements over a wide range of overvoltages to determine the reorganization energy. The described experiments were free from the uncompensated iR drop and charging current problems typical for conventional techniques, the possible perturbation of the ITIES by the externally applied voltage did not occur, and uncertainty in the value of the local electrical potential at the ET site was less important. For modified solid electrodes, one can often find the location of the heterogeneous chemical or electrochemical reaction from the shape of the tip current−distance curve.[20] A similar analysis for an ITIES would be more challenging and would require the use of a much smaller tip electrode, because the combined thicknesses of the mixed-solvent layer and the reaction layers in both solvents is probably less than 10 nm. Studies of the dependence of the rates of ET and IT on the properties of individual solvents and their mutual solubility, along with a more detailed characterization of the interfacial structure, are currently underway in our laboratories.

Formation of a micrometer-thick layer of aqueous solution inside the organic layer (Figure 1C) was observed in several experiments. This tip/electrolyte/substrate configuration operates as a twin-electrode thin-layer cell (TLC) whose thickness can be evaluated from the diffusion limiting current. Electrochemical measurements inside such a TLC, e.g., steady-state voltammetry, can yield kinetic and thermodynamic parameters for the related redox reaction.[15]

SECM can also be used to monitor directly ionic fluxes and electrically neutral molecules. It should be suitable for the study of interfacial transport of such species as O_2, glucose, and drugs across the liquid/liquid interface itself and across a molecular monolayer or bilayer adsorbed at the ITIES.

Acknowledgment. The support of this work by the National Science Foundation and the Robert A. Welch Foundation (A.J.B., C.W.) and the partial support by the donors of the Petroleum Research Fund, administrated by the American Chemical Society (M.V.M.), are gratefully acknowledged. We

thank R. A. Marcus for sending us preprints of his work. Discussions of the ion transfer problem with J. Leddy, T. Solomon, and S. Feldberg were enlightening and helpful.

References and Notes

(1) For reviews of the electrochemistry of ITIES, see: (a) Girault, H. H.; Schiffrin, D. J. In *Electroanalytical Chemistry*; Bard, A. J., Ed.; Marcel Dekker: New York, 1989; Vol. 15, p 1. (b) Senda, M.; Kakiuchi, T.; Osakai, T. *Electrochim. Acta* **1991**, *36*, 253. (c) Girault, H. H. In *Modern Aspects of Electrochemistry*; Bockris J. O'M., Conway, B. E., White, R. E., Eds.; Plenum Press: New York, 1993; Vol. 25, p 1.

(2) (a) Marcus, R. A. *J. Phys. Chem.* **1990**, *94*, 1050. (b) Marcus, R. A. *J. Phys. Chem.* **1990**, *94*, 4155. (c) Marcus, R. A. *J. Phys. Chem.* **1990**, *94*, 7742. (d) Marcus, R. A. *J. Phys. Chem.* **1991**, *95*, 2010. (e) Marcus, R. A. *J. Phys. Chem.* **1995**, *99*, 5742.

(3) Yudi, L. M.; Baruzzi, A. M.; Solis, V. *J. Electroanal. Chem.* **1993**, *360*, 211.

(4) (a) Girault, H. H.; Schiffrin, D. J. In *Charge and Field Effects in Biosystems*; Allen, M. J.; Usherwood, P. N. R., Eds.; Abacus Press: Turnbridge Wells, England, 1984; p 171. (b) Ohkouchi T.; Kakutani, T.; Senda, M. *Bioelectrochem. Bioenerg.* **1991**, *25*, 71, 81.

(5) (a) Kharkats, Yu. I.; Volkov, A. G. *J. Electroanal. Chem.* **1985**, *184*, 435. (b) Kharkats, Yu. I.; Ulstrup, J. *J. Electroanal. Chem.* **1991**, *308*, 71.

(6) Girault, H. H.; Schiffrin, D. J. *J. Electroanal. Chem.* **1988**, *244*, 15.

(7) Guainazzi, M.; Silvestry, G.; Survalle, G. *J. Chem. Soc., Chem. Commun.* **1975**, 200.

(8) (a) Samec, Z.; Marecek, V.; Weber, J. *J. Electroanal. Chem.* **1979**, *96*, 245. (b) Samec, Z.; Marecek, V.; Weber, J. *J. Electroanal. Chem.* **1979**, *103*, 11.

(9) (a) Geblewicz, G.; Schiffrin, D. J. *J. Electroanal. Chem.* **1988**, *244*, 27. (b) Cunnane, V. J.; Schiffrin, D. J.; Beltran, C.; Geblewicz, G.; Solomon, T. *J. Electroanal. Chem.* **1988**, *247*, 203. (c) Cheng, Y.; Schiffrin, D. J. *J. Electroanal. Chem.* **1991**, *314*, 153.

(10) Samec, Z.; Marecek, V. *J. Electroanal. Chem.* **1986**, *200*, 17.

(11) For recent reviews of the SECM see: (a) Bard, A. J.; Fan, F.-R. F.; Mirkin, M. V. In *Electroanalytical Chemistry*; Bard, A. J., Ed.; Marcel Dekker: New York, 1994; Vol. 18, p 243. (b) Bard, A. J.; Fan, F.-R. F.; Mirkin, M. V. *In Physical Electrochemistry: Principles, Methods and Applications*; Rubinstein, I., Ed.; Marcel Dekker: New York, 1995.

(12) Mirkin, M. V.; Richards, T. C.; Bard, A. J. *J. Phys. Chem.* **1993**, *97*, 7672.

(13) (a) Lee, C.; Bard, A. J. *Anal. Chem.* **1990**, *62*, 1906. (b) Jeon, I. C.; Anson, F. C. *Anal. Chem.* **1992**, *64*, 2021.

(14) (a) Scott, E. R.; White, H. S.; Phipps, J. B. *Anal. Chem.* **1993**, *65*, 1537. (b) Horrocks, B. R.; Mirkin, M. V.; Pierce, D. T.; Bard, A. J.; Nagy, G.; Toth, K. *Anal. Chem.* **1993**, *65*, 1213. (c) Wei, C.; Bard, A. J.; Nagy, G.; Toth, K. *Anal. Chem.* **1995**, *67*, 1346.

(15) (a) Mirkin, M. V.; Bard, A. J. *J. Electrochem. Soc.* **1992**, *139*, 3535. (b) Mirkin, V. M.; Bulhões, L. O. S.; Bard, A. J. *J. Am. Chem. Soc.* **1993**, *115*, 201. (c) Mirkin, M. V.; Bard, A. J. Unpublished results.

(16) Bard, A. J.; Fan, F.-R. F.; Kwak, J.; Lev, O. *Anal. Chem.* **1989**, *61*, 1794.

(17) Wipf, D. O.; Bard, A. J. *J. Electrochem. Soc.* **1991**, *138*, 469.

(18) Bruckner-Lea, C.; Janata, J.; Conroy, J.; Pungor, A.; Caldwell, K. *Langmuir* **1993**, *9*, 3612.

(19) Kwak, J.; Bard, A. J. *Anal. Chem.* **1989**, *61*, 1221.

(20) (a) Mirkin, M. V.; Arca, M.; Bard, A. J. *J. Phys. Chem.* **1993**, *97*, 10790. (b) Arca, M.; Mirkin, M. V.; Bard, A. J. *J. Phys. Chem.* **1995**, *99*, 5040.

(21) (a) Nakatani, K.; Uchida, T.; Misawa, H.; Kitamura, N.; Masuhara, H. *J. Phys. Chem.* **1993**, *97*, 5197. (b) Nakatani, K.; Uchida, T.; Misawa, H.; Kitamura, N.; Masuhara, H. *J. Electroanal. Chem.* **1994**, *367*, 109. (c) Nakatani, K.; Uchida, T.; Kitamura, N.; Masuhara, H. *J. Electroanal. Chem.* **1994**, *375*, 387.

(22) Andrieux, C. P.; Savéant, J.-M. In *Molecular Design of Surfaces*; Murray, R. W., Ed.; John Wiley & Sons: New York, 1992; p 207.

(23) Bard, A. J.; Mirkin, M. V.; Unwin, P. R.; Wipf, D. O. *J. Phys. Chem.* **1992**, *96*, 1861.

(24) Wightman, R. M.; Wipf, D. O. In *Electroanalytical Chemistry*; Bard, A. J., Ed.; Marcel Dekker: New York, 1989; Vol. 15, p 267.

(25) Mirkin, M. V.; Fan, F.-R. F.; Bard, A. J. *J. Electroanal. Chem.* **1992**, *328*, 47.

(26) Hanzlik, J.; Samec, Z.; Hororka, J. *J. Electroanal. Chem.* **1987**, *216*, 303.

(27) Karpfen, F. M.; Randles, J. E. B. *Trans. Faraday Soc.* **1953**, *49*, 823.

(28) Nicholson, R. S. *Anal. Chem.* **1965**, *37*, 1351.

(29) Huang, W.; McCreery, R. *J. Electroanal. Chem.* **1992**, *326*, 1.

(30) Kakiuchi, T.; Senda, M. *Bull. Chem. Soc. Jpn.* **1983**, *56*, 2912.

(31) Reid, J. D.; Melroy, O. R.; Buck, R. P. *J. Electroanal. Chem.* **1983**, *147*, 71.

(32) Shao, Y.; Campbell, J. A.; Girault, H. H. *J. Electroanal. Chem.* **1991**, *300*, 415.

(33) Samec, Z.; Marecek, V.; Homolka, D. *J. Electroanal. Chem.* **1981**, *126*, 121.

(34) Marcus, R. A. *J. Chem. Phys.* **1965**, *43*, 679.

(35) Penner, R. M.; Heben, M. J.; Longin, T. L.; Lewis, N. S. *Science* **1990**, *250*, 1118.

(36) (a) Baranski, A. S. *J. Electroanal. Chem.* **1991**, *307*, 287. (b) Oldham, K. B. *Anal. Chem.* **1992**, *64*, 646. (c) Weaver, M. J. *In Electrified Interfaces in Physics, Chemistry and Biology*; Guidelli, R., Ed.; Kluwer Academic Publishers: Dordrecht, Netherlands, 1992; p 427.

(37) Mirkin, M. V.; Bard, A. J. *Anal. Chem.* **1992**, *64*, 2293.

(38) Weaver, M. J. *Chem. Rev.* **1992**, *92*, 463.

(39) Maksymiuk, K.; Doblhofer, K. *Electrochim. Acta* **1994**, *39*, 217.

(40) Gerin, M.; Fresco, J. *Anal. Chim. Acta* **1978**, *97*, 165.

(41) Murray, R. W. In *Electroanalytical Chemistry*; Bard, A. J., Ed.; Marcel Dekker: New York, 1984; Vol. 13, p 191.

JP951278U